Data Repository 2011178

for

Geologic evidence for two pre-2004 earthquakes during recent centuries near Port Blair, South Andaman Island, India

Javed N. Malik[1], M. Shishikura[2], T. Echigo[3], Y. Ikeda[4], K. Satake[5], H. Kayanne[4], Y. Sawai[2], C. V. R. Murty[1] and O. Dikshit[1]

[1]Department of Civil Engineering, Indian Institute of Technology Kanpur, Kanpur 208016. INDIA; E-mail: javed@iitk.ac.in

[2]Active Fault Research Center, AIST, Site C7, 1-1-1 Higashi, Tsukuba 305-8567, JAPAN; E-mail: m.shishikura@aist.go.jp

[3]Geo-Research Institute, 4-3-2, Itachibori, Nishi-ku, Osaka 550-0012, JAPAN. E-mail: echigo@geor.or.jp

[4]Department of Earth and Planetary Sciences, University of Tokyo, Hongo 7-3-1, Bunkyo-ku, Tokyo 113-0033, JAPAN; E-mail: ikeda@eps.s.u-tokyo.ac.jp

[5]Earthquake Research Institute, The University of Tokyo, 1-1-1, Yayoi, Bunkyo-ku. Tokyo 113-0032, JAPAN; E-mail: satake@eri.u-tokyo.ac.jp

Introduction

This Data Repository contains the following information: I: Details of past and present seismicity and crustal deformation based on literature and tide gauge data at Port Blair; II. Details of study site, Mitha-Kadhi, and method, III: Description of all geoslices and trenches. The above information is to supplement the main text and figures.

Item DR-I: Past and Present Seismicity and Crustal Deformation

Recent global plate motion data suggest that the northeast-moving Indian plate converges obliquely at 40 mm/yr with respect to the Sunda micro plate off Sumatra Island near the 2004 epicenter (Paul et al., 2001; Vigny et al., 2005). The recurrence interval inferred from the GPS measurements for large magnitude earthquakes for the Andaman and Nicobar Islands are quite variable: 420-1000 yrs near Andaman Islands (Stein and Okal, 2007) and 140-420 yrs off Sumatra Islands (Chlieh et al., 2007). Further north near the Arakan subduction zone, an Mw 8.5 earthquake every century has been inferred (Socquet et al., 2006).

Past seismicity in the Andaman and Nicobar Islands has been recorded in historical documents (Iyengar et al., 1999; Oritz and Bilham, 2003; Bilham et al., 2005, Rajendran et al., 2007). Large earthquakes occurred on 28 January 1679 (M=7.5?), 31 October 1847 (Mw=7.5-7.9), 31 December 1881 (Mw=7.9), and 26 June 1941 (Mw=7.7) (Figure 1a). Apart from these large earthquakes, several small to moderate events with $4 \leq M \leq 7$ have been observed along the trench and along the Andaman spreading center, varying depths ranging 10-150 km (e.g., Eguchi et al., 1979; Mukhopadhyay 1984; Ortiz and Bilham, 2003; Kayal et al., 2004).

Historical data suggest that land-level changes and tsunamis were generated by a few past earthquakes (Ortiz and Bilham, 2003). The 1881 event generated a tsunami with a maximum height of about 0.8 m, which was recorded at several tide gauge stations around

Bay of Bengal (Ortiz and Bilham, 2003; Bilham et al., 2005). This event caused uplift of Car Nicobar by 0.5 m along the west coast and subsidence by a few centimeters in the eastern part (Bilham et al., 2005). The 1941 event caused uplift of about 1.5 m in Middle Andaman Island along the western coast and the same amount of subsidence along the eastern coast (Jhingran, 1953), however, this data has not been supported by direct measurements (Rajendran et al., 2007). Geomorphic evidences of drowned shorelines along east coast of Andaman Islands are indicative of older events of subsidence (Ortiz and Bilham, 2003).

Tide gauge data at Port Blair during the period from 1916 to 1964, despite non-availability of data between 1921 and 1952, indicate sea level rise at a rate of 2.2 ± 0.5 mm/yr (Figure DR1). Recent submergence during historic times are evidenced also by (1) relicts of an old British settlement at Port Blair that were drowned during the period from 1789 to 1857 (Mouat et al., 1858, cited by Oldham, 1884, and Bilham et al., 2005), and (2) drowned forests in Havelock Island, 40 km northeast of Port Blair (Oldham, 1884). We suggest that these changes in sea level can be attributed to interseismic subsidence. On the other hand, long-term net uplift is inferred from marine terraces (Rajendran et al., 2007; Rajendran et al., 2008). Oldham (1884) also observed the raised marine terrace in the southern part of the Andaman Islands.

The 2004 earthquake resulted in a significant land-level changes along the Sumatra-Andaman arc (Malik and Murty, 2005; Earnest et al., 2005; Meltzner et al., 2006; Tobita et al., 2006; Singh et al., 2006; Kayanne et al., 2007). Large uplift of more than 1 m occurred along the west coasts of the Andaman Islands, whereas a wide zone of subsidence occurred on the backarc side with its axis near Port Blair, where 0.95 m of coseismic subsidence was measured by tidal observations (Singh et al., 2006). The zone of subsidence, which occurs above the down-dip edge of the source rupture, is traceable farther south to Great Nicobar Island where the maximum subsidence of about 3 m was observed (Malik and Murty, 2005).

GPS measurements made before and after the 2004 event in the Andaman and Nicobar Islands indicate coseismic horizontal ground displacement of about 1.5–6.5 m towards SW and coseismic vertical displacement of about 0.5-2.8 m mainly subsidence (Gahalaut et al., 2006). On the basis of these GPS data, slip on the fault is estimated as 3.8–7.9 m beneath the Andaman Islands and about 11-15 m below the Nicobar Islands (Gahaluat et al., 2006). Inversion of tsunami waveforms indicates a similarly large slip, up to 7m, near the Nicobar Islands, while little slip was inferred near the Andaman Islands (Fujii and Satake, 2007).

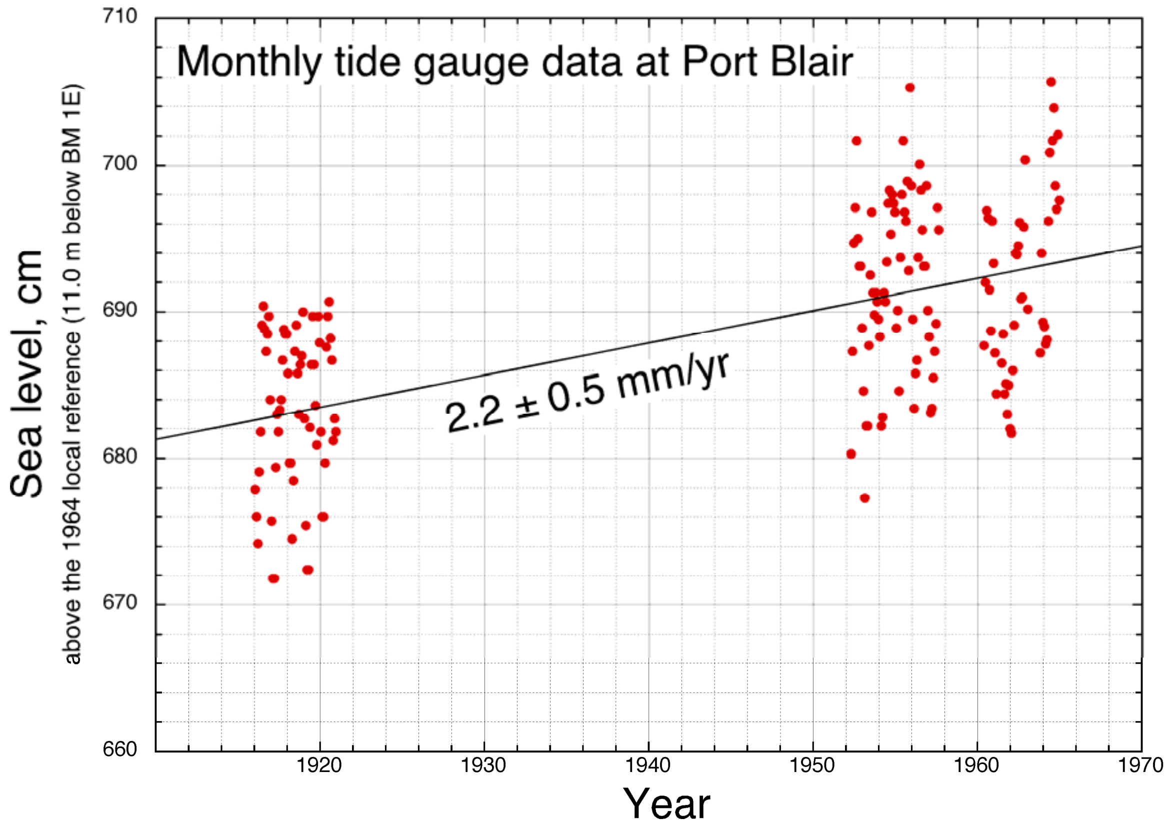

Figure DR1. Graph showing the monthly-averaged tidal data from Port Blair during the period from 1916 to 1964. The data for the period between 1921 and 1952 was not available. The plots indicate sea level rise at a rate of 2.2 ± 0.5 mm/yr. The data is from the Permanent Service of Mean Sea Level (PSML) hosted by the Proudman Oceanographic Laboratory, the Natural Environmental Council, UK (http://www.pol.ac.uk/psmsl/).

Item DR-II: Details of Study Site and Method

The study area around Mitha-Khadi on the western side of the Flat Bay, northwest of Port Blair in South Andaman is located about 10 km inland from the open sea in the east (Figure DR2). Therefore, the area experiencing tropical storms is almost negligible. This was one of the reasons for selecting the site for present study. Also another reason for preferring this area was because it experienced subsidence of ~1 m during the 2004 Sumatra-Andaman earthquake. Therefore, it was presumed that if similar event has occurred in the past then the signatures will be preserved in the stratigraphy without much of alterations.

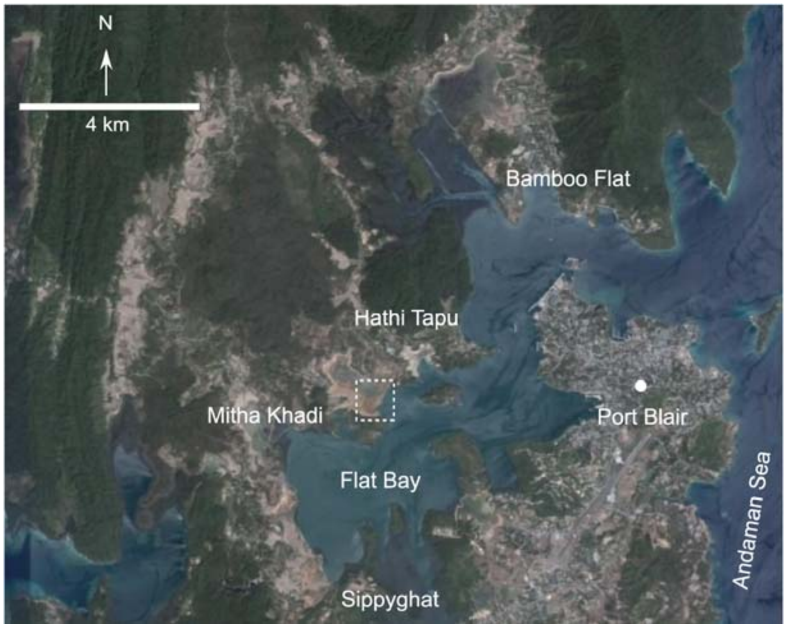

Figure DR2: Google earth image showing regional setting of the area around Port Blair

The Mitha-Khadi area was a back-barrier tidal flat drained by E-W trending tidal channel (Figure 1d, and Supplementary DR3a and d), and bordered on its east by a N-S striking sandy beach ridge, as revealed by about 200 m long E to W topographic profile (Figures 1d and 2). An artificial embankment of about 1-1.5 m above MSL (Mean Sea Level) before the 2004 earthquake prevented the area being flooded during the high tides, hence was used for farming before the 2004 event (Figure DR 3c). However, after the area experienced subsidence of about ~ 1 m during the 2004 earthquake, the beach ridge area is about 0.5 m above the MSL, and is frequently inundated by the high tides. To protect the area from inundation the embankment is again raised by about 1.5 m after the 2004 event (Figure DR3a).

Figure DR3.

(a) To protect the area from the inundation by sea water during high tides an artificial embankment was constructed around AD 1800 by British. The same wall was raised by ~ 1.5 m after the 2004 Sumatra-Andaman earthquake because of coseismic subsidence. View of the photo looking east.

(b) The survivors informed us that a 3.0-3.5 m high tsunami wave in 2004 inundated the area up to about 1.5 km inland around Mitha-Khadi.

(c) Paddy crops laid down in NW direction by the tsunami wave entering the area from the Flat Bay side.

(d) A view looking east shows an E-W flowing tidal channel in the right hand side of the photo. Embankment runs parallel in N-S direction bordering the bay area, and along the banks of the E-W flowing tidal channel.

Paleo-botanical signatures and environment of Mitha Khadi in past:

It is presumed that before the construction of the artificial embankment across the tidal flats (wall trends in N-S direction), this area was probably occupied by mangroves forest. This can be envisaged based on the presence of mangroves in the nearby tidal flats along the bay region. The construction of the wall was during Britisher's period i.e. ~ AD 1800. During this period the mangroves forests were probably converted into farming land (Figures D3 a-d).

Methods:

Shallow water table prevented us from trenching deeper than 1.5 m in depth. In order to get deeper stratigraphic sections, we used a soil sampler called geoslicer (Nakata and

Shimazaki, 1997), this model extracts flat-platy core samples 1.5 m long, 12 cm wide and 2.0 cm thick.

Diatom subsample spanned about 1 cm and were prepared for glass slides using sodium hypochlorite solution (Sawai et al., 2009). We counted 20-150 diatom valves in the prepared slides from clay–peaty silt samples. To infer autecology of diatom species, we referred standard reference for freshwater and brackish diatoms (e.g., Vos and deWolf, 1993; Witkowski et al., 2000).

Item DR-III: Description of Geoslice and Trench Samples:

North Trench (T1) excavated during May 2005. The exposed east wall of the N-S trench shows four units (*d* to *a*). Unit *d* (older) comprise of massive bluish gray clayey-silt with sand-intrusion marked by yellowish medium to fine sand. This unit is fractured due to multiple intrusions of sand dykes. Unit *c* is marked with sharp contact with the underlying unit *d*. It shows chaotic nature with mud clasts + sandy matrix and prominent laminations in the upper part. Unit *b* shows erosive and sharp contact with underlying unit *c*. Unit *b* indicates probable tsunami deposit; it shows medium to coarse sand at the base overlain by thinly laminated mud and silty sand, and sand with abundant reworked mud clast near the top. This sequence probably marks deposition by more than one wave, but not distinctly revealed from the succession. Deposition of coarse sand indicates deposition by strong tsunami wave, followed by deposition of laminated unit by weaker waves. This unit is devoid of bio-turbation.

Figure DR4a. East wall view of T1 trench

North Trench (T2) was excavated during March 2006. West wall revealed fractured unit *d* at the bottom part of the trench, intruded by sand and sand blow with mud clasts. Prominent unconformity is observed between unit *c* and the overlying tsunami deposits (unit *b*). Unit *c* shows chaotic nature with abundant mud clasts and poor lamination occasionally. Unit *b* shows alternate sequence of medium to coarse sand and lamination of mud and silty sand. Number 1 and 2 marks the location of charred peaty material dated from unit *c* at around 1686-1496 BC and 2400-2200 BC respectively (Table DR1).

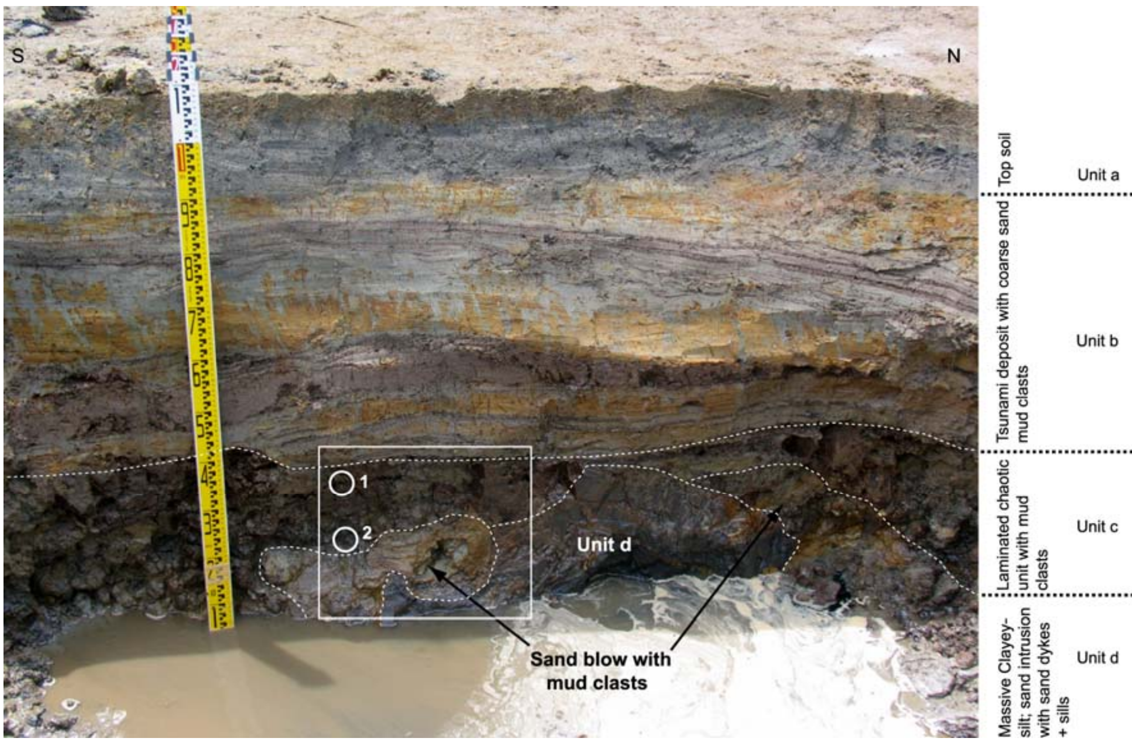

Figure DR4b. West wall of T2 trench

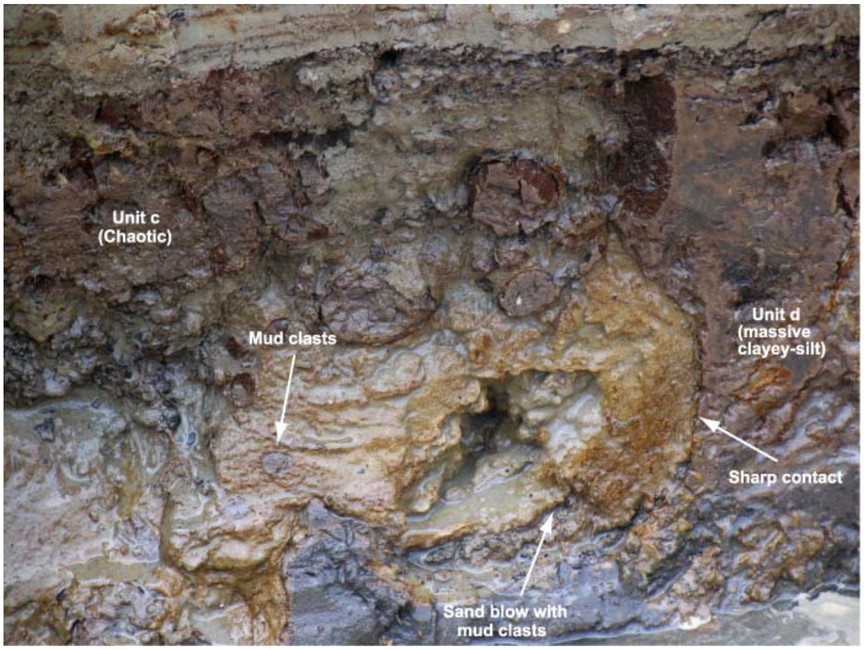

Figure DR4c: Close-up view of sand blow. The contact between the sand blow and unit *d* is very sharp. The shows engulfed mud clasts.

We dated total 5 samples of rhizomes from unit *e*, two samples from north trench, two samples from M2 and one from M3. The ages obtained from these samples range from AD 1680-1950 to AD 250-530. The ages obtained from the boundary between units *d* and *e*, i.e. from the geoslices M2 at a depth of 119 cm and M3 at depth of 144 cm are AD 1670-1950 and AD 1670-1950. Two samples (nos. 1 and 2 as listed in Figure DR4d) from T2-geoslice gave age of AD 1680-1950 (depth 140 cm) and AD 1520-1950 (depth of 160 cm). The ages of the rhizomes obtained from T2-geoclice, M2 and M3 are well constrained (~AD 1670). This is because the root of plant does not extend upward, but rather gets terminated/sharply at the depth of about 1.5 m below the surface.

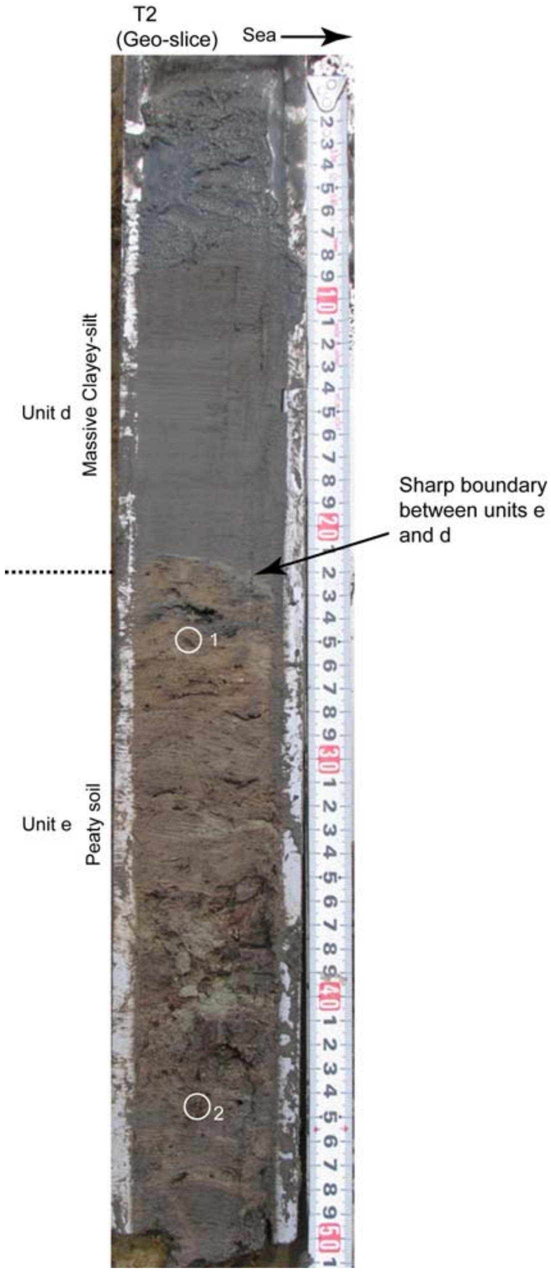

Figure DR4d: Geoslice section from north trench (T2) excavated in March 2006. This section was collected from about 120 cm below the surface. Sharp contact between unit *e* and overlying unit *d* is noticed. White circles shows location of samples

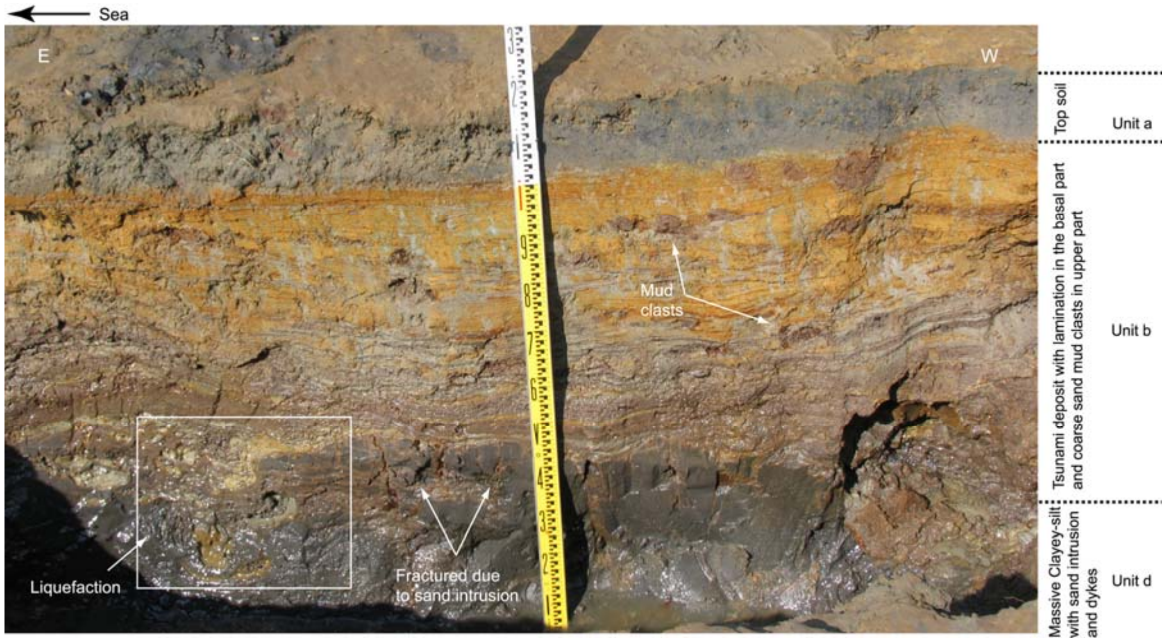

Figure DR5a: South wall of north trench T3 (excavated during December 2006) showing distinct units from *d*, *b* and *a*.

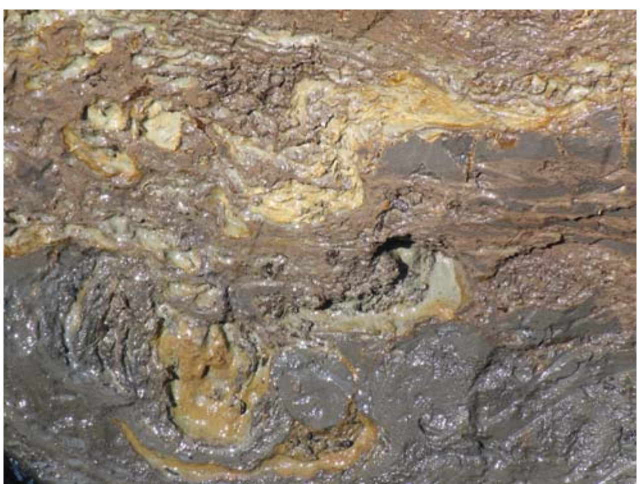

Figure D5b: Close-up view of sand intrusion and convolution formed due to liquefaction.

Trench T4. This trench (T4) was excavated in December 2006 on the left bank of tidal channel (Figure 1d). The exposed section of T4 show units *c*, *b* and *a*. Well preserved inclined stratification (inclination towards land) in unit *b* was observed. This was recorded in M3 and another north trench (T2) excavated in December 2006. The inclined stratification comprised of laminated sequence of mud and silty-sand. In trench T4 a lensoidal body consisting of mud clasts was observed in the middle part.

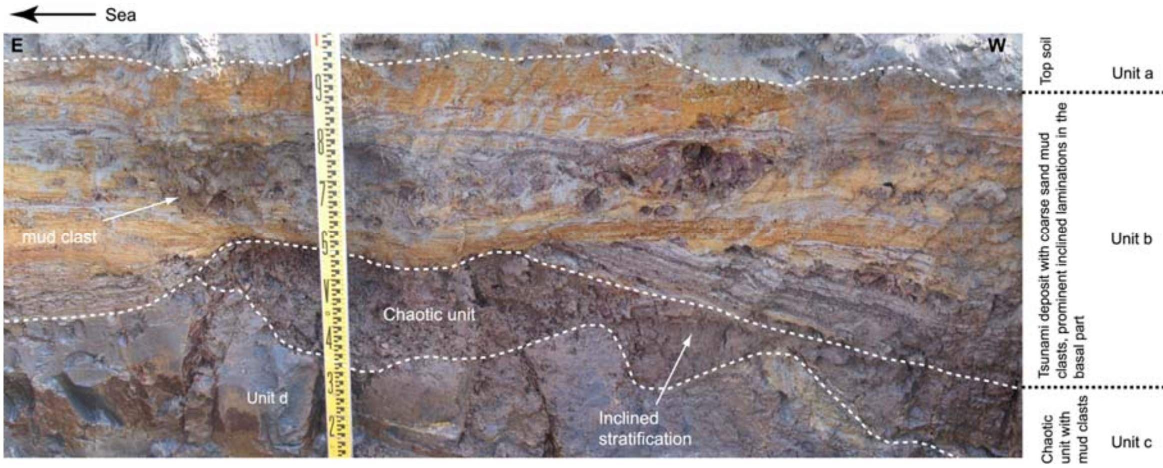

Figure DR6. South wall view of T4 trench excavated in 2006.

Trench T5. South trench T5 was excavated during December 2006 on the right bank of the tidal channel (Figure 1d). The south wall shows distinct units from *c*, *b* and *a*. Lower base of the trench is occupied by unit *c*. This unit is chaotic in nature comprised of mud clasts, shows poor lamination in the upper part. Unit *b* shows sharp non-erosive contact with underlying unit *c*. Unit *b* marks the tsunami deposit.

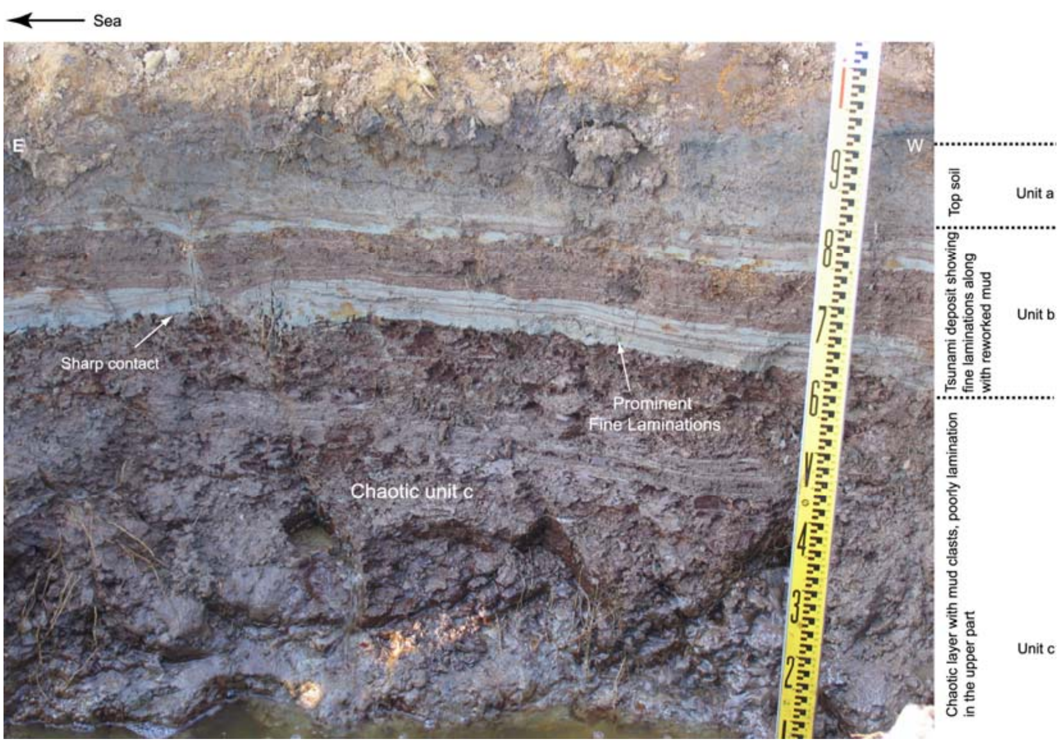

Figure DR7. South wall of south trench T5

Geoslice Sections. Geoslice sections M1 and M2 show unit *b* comprising finer silty-sand deposit with fine laminations. The contact with the underlying unit is sharp to non-erosive. Lamination with reworked peaty material suggests stagnation of water after the strong wave.

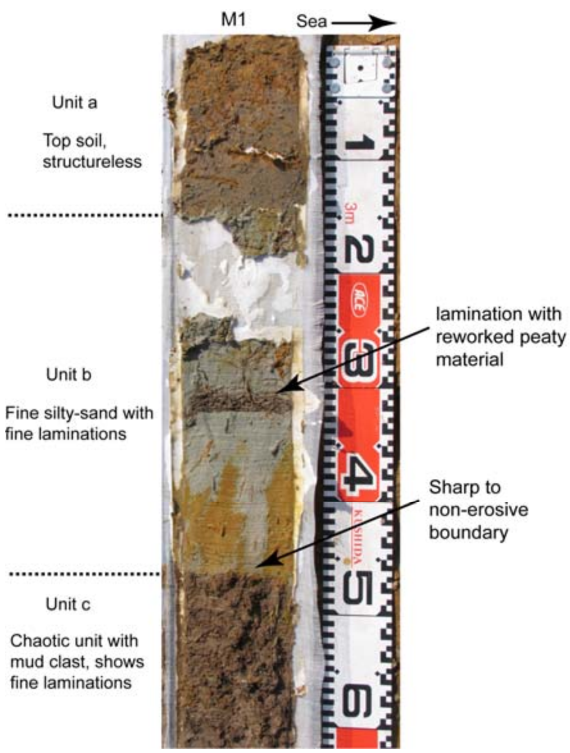

Figure DR8a. The M1 section shows geoslice peel sample.

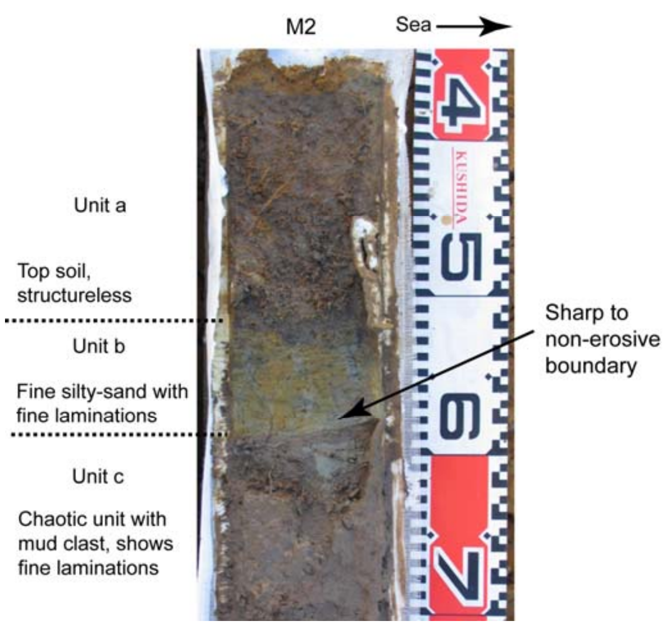

Figure DR8b: M2 section shows geoslice peel sample.

Close-up view of M3 (Figure DR9) shows inclined stratification towards land and sharp and erosive contact with underlying unit *c*. Unit *b* is interpreted as tsunami deposit. Unit *a* is highly disturbed unit due to farming.

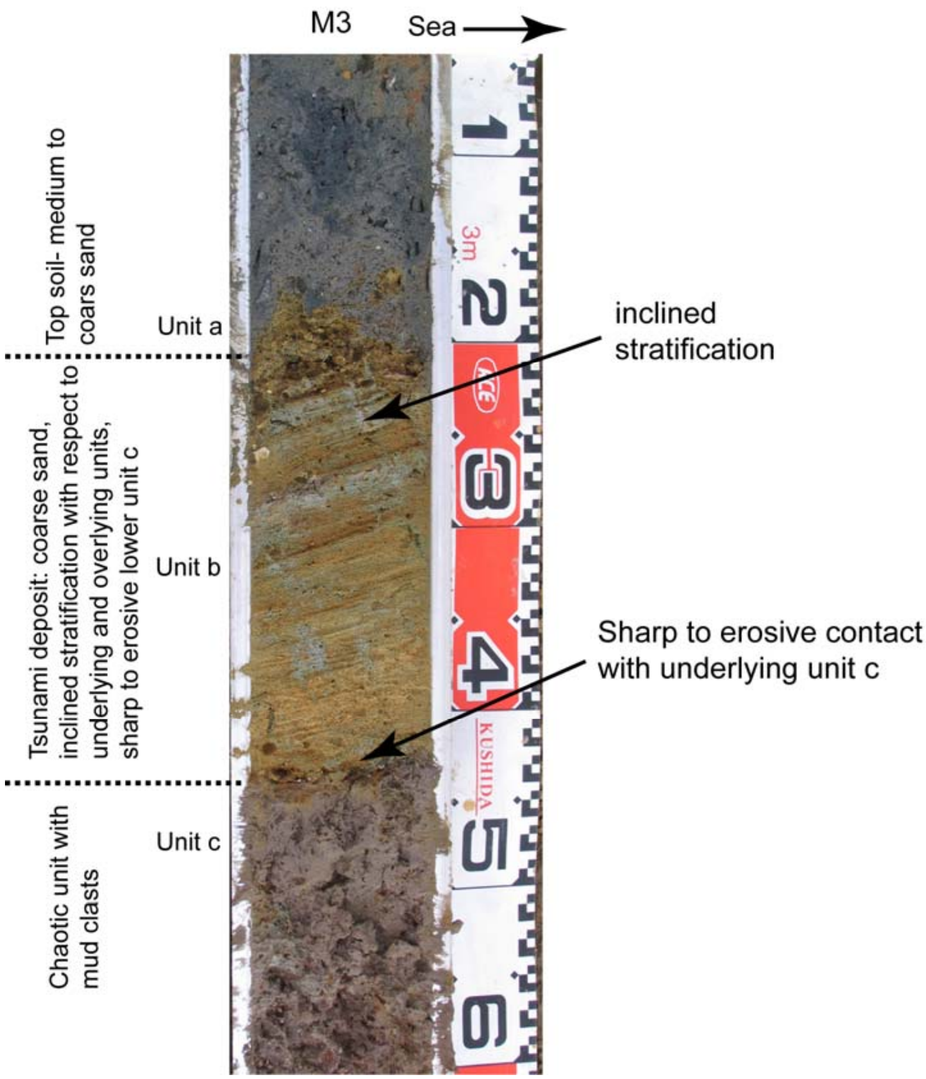

Figure DR9. Close-up view of M3 (geoslice sample)

Geoslice section M4 shows prominent sedimentary features of units *d*, *e* and *f*. Sharp contact is marked between unit *e* and the overlying unit *d*. The plant root (rhizome) shows sharp upward termination at a depth of about 170 cm, suggestive of sudden change in land-level and environment from marshy to sub-tidal. This evidence suggests subsidence occurred due to large earthquake during Event I.

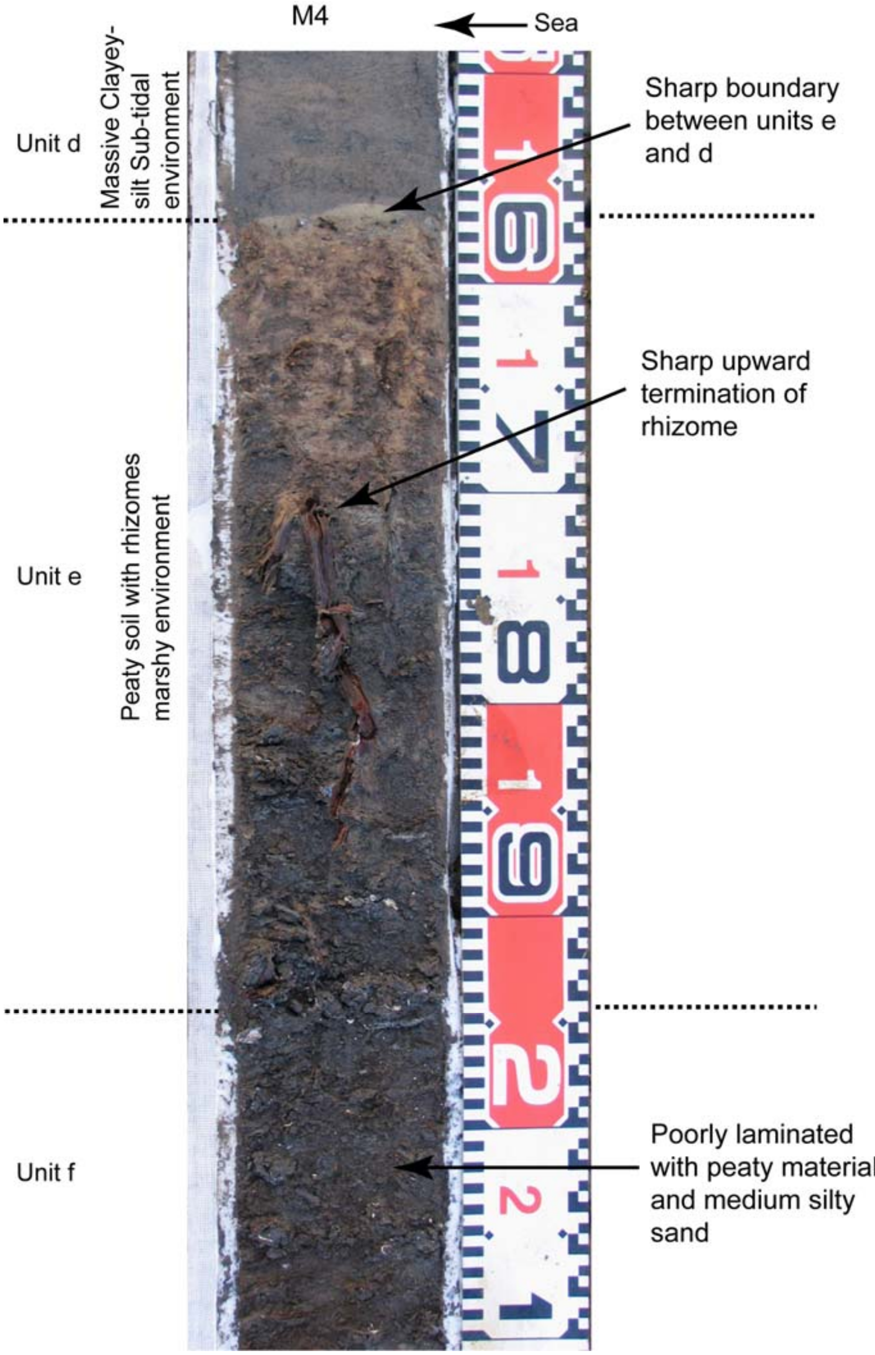

Figure DR10. The M4 section (geoslice sample).

To get paleoecological information during the deposition of units *e* and *d* diatoms analysis were carried from geo-slice M4. Diatom subsamples spanned about 1 cm were analyzed from the bottom and top portion of the units *d* and *e* respectively. We counted 20-150 diatom valves in the prepared slides from clay –peaty silt samples. Fossil diatom assemblages revealed drastic change within unit *e* (Figure 2). In the bottom portion of the unit *e*, a few brackish-marine species *Pseudopodosira westii*, *Tryblionella cocconeiformis*, and *T. compressa* are present. These taxa decrease in middle portion of the unit, and the unit becomes dominated by the other brackish species *Caloneis linearis* and *Diploneis suborbicularis*, this marks unit *d*. Fossil diatom assemblages in the upper portion change to predominance of freshwater-brackish taxa (*Diadesmis contenta*, *Pinnularia spp.*, and *Cosmioneis pusilla*). This vertical change in diatom assemblages implies that the area became emerged from tidal water during the deposition of unit *e*.

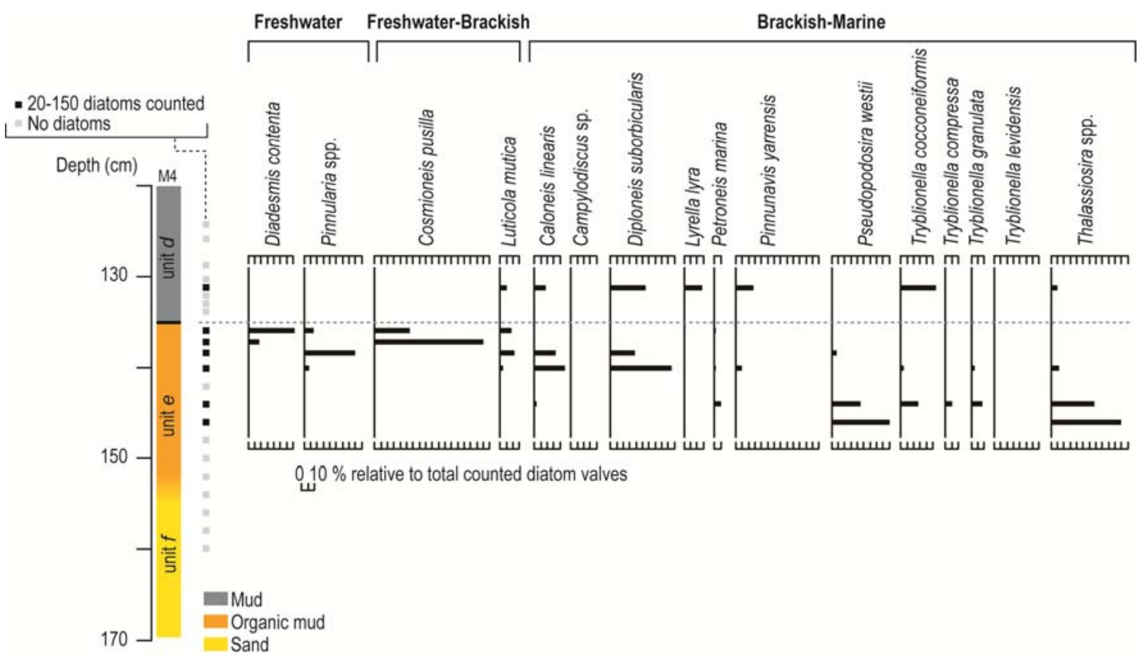

Figure DR11. Diatom analysis of M4

REFERENCES CITED IN DATA REPOSITORY

Bilham, R., Engdahl, E. R., Feldl, N., and Satyabala, S. P., 2005, Partial and Complete Rupture of the Indo-Andaman plate boundary 1847-2004: Seismological Research Letters, v. 76, p. 299-311.

Chlieh, M., Avouac, J. P., Hjorleifsdottir, V., Song, TR. A., Ji, C., Sieh, K., Sladen, A., Hebert, H., Prawirodirdjo, L., Bock, Y., and Galetzka, J., 2007, Coseismic slip and afterslip of the Great (Mw9.15) Sumatra–Andaman Earthquake of 2004: Bulletine of the Seismological Society of American, v. 97, p. 152-173, doi: 10.1785/0120050631.

Earnest, A., Rajendran, C. P., Rajendran, K., Anu, R., Arun, G. M., and Mohan, P. M., 2005, Near-field observations on the co-seismic deformation associated with the 26 December 2004 Andaman-Sumatra earthquake: Current Science, v. 89, p. 1237– 1244.

Eguchi, T., Uyeda, S., and Maki, T., 1979. Seismotectonics and Tectonic History of the Andman Sea: Tectonophysics, v. 57, p. 35-51.

Fujii, Y. and Satake, K., 2007, Tsunami source of the 2004 Sumatra-Andaman earthquake inferred from tide gauge and satellite data: Bull. Seism. Soc. Am., vol. 97., p. S192-S207.

Gahalaut, V. K., Nagarajan, B., Catherine, J. K., and Kumar, S., 2006, Constraints on 2004 Sumatra-Andaman earthquake rupture from GPS measurements in Andaman-Nicobar Islands: Earth and Planetary Science Letters, v. 242, p. 365–374.

Iyengar, R. N., Sharma, D. and Siddiqui, J. M., 1999, Earthquake history of Indian medieval times: Indian Journal of Historical Sciences: v. 34(3), p. 181–237.

Jhingran, A. G., 1953, A note on an earthquake in the Andaman Islands (26th June 1941): Records Geological Survey of India, v. 82, p. 300–307.

Kayal, J. R., Gaonkar, S. G., Chakraborty, G. K., and Singh, O. P., 2004, Aftershocks and seismotectonics implications of the 13 September 2002 earthquake (Mw 6.5) in the Andaman Sea basin: Bulletin of Seismological Society of America, v. 94(1), p. 326–333.

Kayanne, H., Ikeda, Y., Echigo, T., Shishikura, M., Kamataki, T., Satake, K., Malik, J. N., Basir, S. R., Chakrabortty, G. K., and Ghosh Roy, A. K., 2007, Coseismic and postseismic creep in the Andaman Islands associated with the 2004 Sumatra-Andaman Earthquake: Geophysical Research Letter, v. 34, L01310, 10.1029/2006GL028200.

Malik, J. N., and Murty, C. V. R., 2005. Landscape Changes in Andaman & Nicobar Islands (India) due to Mw9.3 Tsunamigenic Sumatra Earthquake of 26 December 2004: Current Science, v. 88(9), p. 1385-1386.

Meltzner, A. J., Sieh, K., Abrams, M., Agnew, D. C., Hudnut, K. W., Avouac, J. P., and Natawidjaja, D. H., 2006, Uplift and subsidence associated with the great Aceh-Andaman earthquake of 2004: Journal Geophysical Research, v. 111, doi:10.1029/2005JB003891.

Mouat, F. J., Playfair G. R., and Heathcote, J. S., 1858, Report by the Andaman Committee to C. Beadon, Secretary to the Government of India, Home Department, dated Port Andaman, 1 Jan 1858.

Mukhopadyay, M., 1984, Seismotectonics of subduction and back-arc rifting under the Andaman Sea: Tectonophysics, v. 108, p. 229–239.

Nakata, T. and Shimazaki, K., 1997, Geo-slicer, a newly invented soil sampler, for high-resolution active fault studies: Journal of Geography (Chigaku zassi), v. 106, p. 59-69 (in Japanese with English abstract).

Oldham, T., 1883, A catalogue of Indian earthquakes from the earliest end of 1869: Memoirs Geological Survey of India, v. 3, p. 1–53.

Ortiz M. and Bilham R., 2003, Source area ad rupture parameters of the 31 December 1881 Mw = 7.9 Car Nicobar earthquake estimated from tsunamis recorded in the Bay of Bengal: Journal Geophysical Research, v. 108, doi:10.1029/2002JB001941.

Paul, J., Burgmann, R., Gaur, V. K., Bilham, R., Larson, K. M., Ananda, M. B., Jade, S., Mukal, M., Anupama, T. S., Satyal, G., and Kumar, D., 2001, The motion and active deformation of India: Geophysical Research Letter, v. 28, p. 647–650.

Rajendran, C. P., Rajendran, K., Earnest, R. A., Machado, T., Mohan, P. M., and Freymueller, J., 2007, Crustal deformation and seismic history asssociated with the 2004 Indian Ocean earthquake: a perspective from the Andaman–Nicobar Islands, Bulletin of Seismological Society of America, v. 97, p. 174-191.

Rajendran, K., Rajendran, C. P., Earnest, A., Ravi Prasad, G.V., Dutta, K., Ray, D. K., Anu, R., 2008, Age estimates of coastal terraces in the Andaman and Nicobar Islands and their tectonic implications, Tectonophysics, v. 455, p. 53–60.

Reimer, P. J., Baillie, M. G. L., Bard, E., Bayliss, A., Beck, J. W., Blackwell, P. G., Bronk Ramsey, C., Buck, C. E., Burr, G. S., Edwards, R. L., Friedrich, M., Grootes, P. M., Guilderson, T. P., Hajdas, I., Heaton, T. J., Hogg, A. G., Hughen, K. A., Kaiser, K. F., Kromer, B., McCormac, F. G., Manning, S. W., Reimer, R. W., Richards, D. A., Southon, J. R., Talamo, S., Turney, C. S. M., van der Plicht, J., Weyhenmeyer, C. E., 2009, IntCal09 and Marine09 radiocarbon age calibration curves, 0-50,000 years cal BP: Radiocarbon, v. 51, p. 1111-1150.

Sawai, Y., Jankaew, K., Martin, M.E., Choowong, M., Charoentitirat, T., Prendergast, A. (2009) Diatom assemblages in tsunami deposits associated with the 2004 Indian Ocean tsunami at Phra Thong Island, Thailand. Marine Micropaleontology, 73, 70-79.

Singh, S. K., Ortiz, M., Gupta, H. K., and Ramadas, D. G. A., 2006, Slow slip below Port Blair, Andaman, during the great Sumatra-Andaman earthquake of 26 December 2004: Geophysical Research Letter, v. 33, L03313, doi 10.1029/2005GL025025.

Stein, S., and Okal, E. A., 2007, Ultralong Period Seismic Study of the December 2004 Indian Ocean Earthquake and Implications for Regional Tectonics and the Subduction Process: Bulletin of the Seismological Society of America, v. 97, No. 1A, pp. S279–S295, doi: 10.1785/0120050617.

Vos, P. C. and deWolf, H., 1993. Diatoms as a tool for reconstructing sedimentary environments in coastal wetlamd; methodological aspects. Hydrobiologia, v. 269/270, p. 285-296.

Witkowski, A., Lange-Bertalot, H. and Metzeltin, D., 2000. Diatom flora of marine coasts I. Iconographia Diatomologica Vol. 7. 925pp. A.R.G. Gantner Verlag K.G., Ruggell.

Vigny, C., Simons, W. J. F. , Abu, S., Bamphenyu, R., Satirapod, C., Choosakul, N., Subarya, C., Socquet, A., Omar, K., Abidin, H. Z., and Ambrosius, B. A. C., 2005, Insight into the 2004 Sumatra-Andaman earthquake from GPS measurements in southwest Asia: Nature, v. 436, p. 201-206.

Table DR1: Radiocarbon dates

Sample No.	Sample site	Depth (cm)	Layer unit	Material	$\delta^{13}C$ (‰)	Conventional age (^{14}C yrs)	Calendar age (2σ)	Lab Code
1	North trench T2	70	c	Charred material	-27.7	3300 ± 40	1686-1496 BC	Beta-217416
2	North trench T2	90	c	Charred material	-26.3	3870 ± 40	2467-2274 BC (88.72 %) 2256-2208 BC (11.28 %)	Beta-217417
3	North trench T2 (Geoslice)	140	e	Plant fragments (rhizome)	-24.4	60 ± 40	AD 1685-1732 (25.96 %) AD 1808-1927 (72.48 %) AD 1951-1954 (1.56 %)	Beta-217418
4	North trench T2 (Geoslice)	160	e	Plant fragments (rhizome)	-27.7	220 ± 40	AD 1525-1557 (3.14 %) AD 1631-1695 (35.16 %) AD 1726-1813 (46.48 %) AD 1838-1842 (0.17 %) AD 1853-1867 (0.82 %) AD 1874-1875 (0.05 %) AD 1918-1952 (14.19 %)	Beta-217419
5	M1 geoslice	30	b	Charred material	-31.1	580 ± 40	AD 1297-1373 (65.11 %) AD 1377-1422 (34.89 %)	Beta-228221
6	M1 geoslice	98	d	Charred material	-27.9	130 ± 40	AD 1670-1780 (41.35 %) AD 1798-1896 (41.59 %) AD 1902-1944 (16.08 %) AD 1950-1953 (0.98 %)	Beta-228222
7	M1 geoslice	130	e	Charred material	-28.9	2030 ± 40	164-129 BC (7.85 %) 120 BC- AD 57 (92.15 %)	Beta-228223
8	M2 geoslice	119	e	Plant fragments (rhizome)	-26.0	140 ± 40	AD 1668-1782 (44.71 %) AD 1797-1893 (37.96 %) AD 1905-1948 (16.70 %) AD 1950-1953 (0.62%)	Beta-241412
9	M2 geoslice	144	e	Plant fragments (rhizome)	-29.5	1670 ± 40	AD 254-437 (95.30 %) AD 488-512 (3.05 %) AD 516-530 (1.65 %)	Beta-241413

10	M3 geoslice	132	e	Plant fragments (rhizome)	-27.1	150 ± 40	AD 1666-1784 (48.11 %) AD 1795-1892 (33.92 %) AD 1908-1953 (17.97 %)	Beta-228224
11	M3 geoslice	144	e	Charred material	-28.2	1130 ± 40	AD 780-792 (2.86 %) AD 803-992 (97.14 %)	Beta-228225
12	M4 geoslice	193	e	Shell fragments	-0.7	1570 ± 40	AD 708-925	Beta-228226
13	M4 geoslice	261	f	Charred material	-28.2	1950 ± 40	40 BC- AD 128	Beta-228227
14	M5 geoslice	55	b	Charred material	-30.2	3220 ± 40	1607-1570 BC (8.62 %) 1561-1546 BC (2.41 %) 1541-1417 BC (88.97 %)	Beta-228228
15	M5 geoslice	122	?	Charred material	-26.2	2010 ± 40	154-139 BC (1.84 %) 112 BC- AD 74 (98.16 %)	Beta-228229

Calendar ages were calculated using IntCal 09 and Marine09 (Reimer et al., 2009). Delta R of marine reservoir correction for shell sample was regarded to be 0.
AMS dating was carried out at Beta Analytic Inc., USA.